INVESTIGATING THE EFFECTS OF ROUGHNESS ELEMENTS OF A WING PROFILE ON THE INTENSITY OF HEAT TRANSFER

V. M. Buznik, G. A. Artemov, V. N. Bandura, and A. M. Fedorovskii

Inzhenerno-Fizicheskii Zhurnal, Vol. 14, No. 3, pp. 460–469, 1968

UDC 536.244

We present the results of an investigation into the roughness elements of a wing profile on the transfer of heat and aerodynamic resistance of a plate and a tubular surface. Criterial formulas have been derived for the calculation of the heat transfer and resistance. An evaluation of the efficiency of these tubes has demonstrated that knurling the roughness elements will serve to reduce the heat-transfer surface by 40% relative to that of a smooth surface.

The roughening of a heat-transfer surface represents one method of enhancing heat transfer. The purpose of producing roughness elements is to disrupt the boundary layer. On the one hand, the disruption of the boundary layer leads to a reduction in its thermal resistance, while on the other hand, it caused the hydraulic losses to increase. It is therefore necessary to seek the most advantageous relationship between the increase in heat transfer and resistance. A study of the intensification of heat transfer from plate and tubular surfaces is therefore of practical interest.

Let us consider an approximate solution for the problem of heat transfer from a plate with a solitary roughness element. Let the plate with the solitary roughness element be streamlined by an nonisothermal incompressible fluid exhibiting constant physical properties. The integral boundary-layer equation in this case will have the form

$$\frac{d\delta_t^{**}}{dx}+\left[\frac{W'}{W}-\frac{\theta'}{\theta}\right]\delta_t^{**}=\frac{q_w}{c_p\gamma W\theta}\ . \tag{1}$$

We will use the approximate solution of Eq. (1) proposed by Ambrok [1]. The Ambrok method is based on the assumption that the heat-transfer law is independent of the pressure gradient, as well as of the surface temperature. The heat-transfer law is understood to refer to a functional relationship of the following form:

$$\frac{q_w}{c_p\gamma W\theta}=f(\mathrm{Re}_t^{**}). \tag{2}$$

The law is sought for a plate with a constant wall temperature ($W' = 0$; $\theta' = 0$) with consideration of the criterial relationship

$$\mathrm{Nu}_x=A\,\mathrm{Re}_x^n \tag{3}$$

and has the form

$$\frac{q_w}{c_p\gamma W_\infty\theta}=\left(\frac{n^{n-1}A}{\mathrm{Pr}}\right)^{\frac{1}{n}}\mathrm{Re}^{**\frac{n-1}{n}}\ . \tag{4}$$

With substitution of (4) into Eq. (1) we derive a Bernoulli-type differential equation for the determination of δ_t^{**}:

$$\frac{d\delta_t^{**}}{dx}+\left(\frac{W'}{W}+\frac{\theta'}{\theta}\right)\delta_t^{**}=\left(\frac{n^{n-1}A}{\mathrm{Pr}}\right)^{\frac{1}{n}}\mathrm{Re}_t^{**\frac{n-1}{n}}\ . \tag{5}$$

The general solution for this equation has the form

$$\delta_t=\left[\frac{\left(\frac{A}{n\,\mathrm{Pr}}\right)^{\frac{1}{n}}}{(W\theta)^{\frac{1}{n}}\nu^{\frac{n-1}{n}}}\int_0^x W\theta\,dx+\frac{C_1}{(W\theta)^{\frac{1}{n}}}\right]^n. \tag{6}$$

The integration constant is determined from the following condition: when $x = x_0$, the quantities δ_t^{**}, W, and θ assume specific fixed values, i.e.,

$$C_1=\left(W\theta\delta_t^{**}\right)^{\frac{1}{n}}.$$

If we consider a uniform boundary layer whose origin coincides with the heating origin, we find that $C_1 = 0$ and

$$\delta_t^{**}=\frac{\nu}{W\theta}\left[\left(\frac{A}{n\,\mathrm{Pr}}\right)^{\frac{1}{n}}\int_0^x\frac{W\theta^{\frac{1}{n}}}{\nu}\,dx\right]^n. \tag{7}$$

With consideration of (7), we transform Eq. (1) as follows:

$$\mathrm{Nu}_x=A\,\frac{W_\infty x^n}{\nu^n}\left(\frac{W}{W_\infty}\right)^n\left(\frac{\frac{W}{W_\infty}\theta^{\frac{1}{n}}x}{\int_0^x\frac{W}{W_\infty}\theta^{\frac{1}{n}}\,dx}\right). \tag{8}$$

Formula (8) is equally applicable to the calculation of a boundary layer of any structure. In the derivation of this formula we have imposed a limitation in the sense that a layer of identical structure is assumed to be coincident with the heating origin.

To derive a formula which will make it possible to calculate the transfer of heat in the case of a mixed boundary layer, the value of the arbitrary constant $C_1 = (W\theta\delta_t^{**})^{1/n}$ must be substituted into (6), and we have to take the same steps as when $C_1 = 0$.

Let us consider the case of a completely turbulent boundary layer whose origin coincides with the heating origin. Using the relationship [3]

$$\mathrm{Nu}_x=0.0235\,\mathrm{Re}_x^{0.8} \tag{9}$$

for the heat transfer of a plate with t = const, we transform (8) into a formula for the calculation of the local heat transfer of a plate with a solitary roughness element, given a variable wall temperature

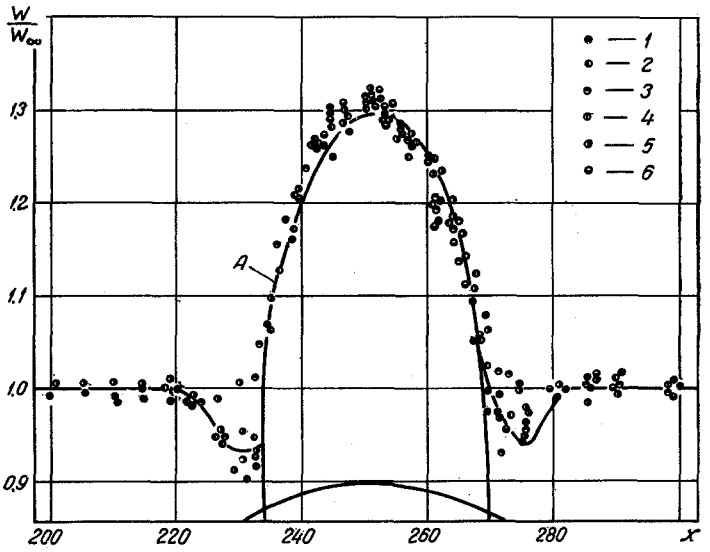

Fig. 1. Distribution of dimensionless velocity beyond the boundary layer along the plate with roughness element No. 2 (x, mm). Velocity of incoming flow W_∞, m/sec: 1) 14; 2) 17; 3) 23.3; 4) 27; 5) 33; 6) 40; A) theoretical curve.

$$\mathrm{Nu}_x = 0.0235\,\mathrm{Re}_x^{0.8}\left(\frac{W}{W_\infty}\right)^{0.8} K_{\text{v.t.r}}, \qquad (10)$$

where

$$K_{\text{v.t.r}} = \left(\frac{\dfrac{W}{W_\infty}\,\theta^{1.25}\,x}{\displaystyle\int_0^x \frac{W}{W_\infty}\,\theta^{1.25}\,dx}\right)^{0.2}. \qquad (11)$$

It is not difficult to see that for convex curves with an indistinct maximum or minimum—which is the case in the streamlining (when q = const at the surface) of a plate with a solitary roughness element—the expression in the parentheses in (11) does not exceed 2, and we will have the inequality

$$1 < K_{\text{v.t.r}} < \sqrt[5]{2} < 1.15.$$

Assuming that $K_{\text{v.t.r}} = 1.08$, we derive a formula for the calculation of the local heat transfer from a plate with a solitary roughness element:

$$\mathrm{Nu}_x = 0.0255\,\mathrm{Re}_x^{0.8}\left(\frac{W}{W_\infty}\right)^{0.8}. \qquad (12)$$

Here we must know the distribution of velocities W/W_∞ at the outside edge of the boundary layer or, correspondingly, the pressure gradient of the potential flow.

The experimental investigation was carried out on an installation which consisted of a square working section 200 · 200 in size, connected to the suction mechanism of a rectangular wind tunnel. With this installation we were able to measure the local temperature of the surface, the velocity distribution in the boundary layer, the distribution of the static pressure at the calorimeter surface, and with the wind-tunnel balance we were able to measure the force of the total plate resistance.

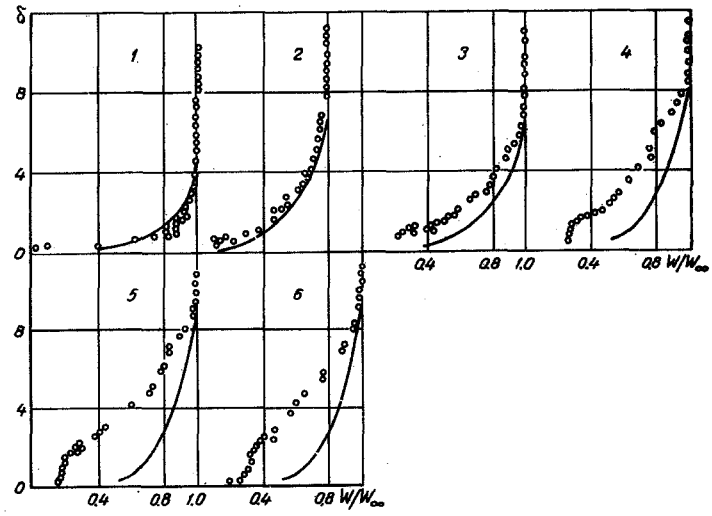

Fig. 2. Velocity diagrams in boundary layer on plate with roughness element No. 3 measured with microtube. Coordinate of section x, mm, with respect to front edge of plate (δ, mm): 1) 254; 2) 261; 3) 266; 4) 271; 5) 281; 6) 289.

The Characteristics of Rough Tubes

Tube number	Roughness-element profile	Profile chord, in mm	Relative knurling pitch
1	$z = z_{f_0} + 1.5z_{c_2}$	12.5	1
2	$z = z_{f_0} + 1.5z_{c_2}$	12.5	2
3	$z = z_{f_0} + 1.5z_{c_2}$	12.5	4
4	$z = z_{f_0} + 1.5z_{c_2}$	16.6	2
5	$z = z_{f_0} + 2z_{c_2}$	12.5	2
6	Half-cylinder	Diameter 3.72	2

The calorimeter plate was designed so as to make possible the replacement of the middle (upper and lower) sections with various inserts: a single smooth insert and three with various roughness elements. The profile characteristics were calculated by the Simonov method [4] according to which the following notation has been adopted for the roughness elements: roughness element No. 1—profile $z = z_{f_0} + 1.2\, z_{c_3}$, chord length b = 50 mm; roughness element No. 2—profile $z = z_{f_0} + 1.2\, z_{c_3}$, chord length b = 35 mm; roughness element No. 3—profile $z = z_{f_0} + 1.5\, z_{c_2}$, chord length b = 35 mm.

Figure 1 shows the results from the measurement of static pressures on a plate with roughness element No. 2. The values of the dimensionless velocity W/W_∞ have been plotted along the axis of ordinates, while the distance from the leading edge of the plate is plotted along the axis of abscissas. The theoretical curve is also plotted here.

To determine the state of the boundary layer at the roughness element and beyond, we measured the velocities in the boundary layer at various cross sections along the length of the plate.

The microtube measurements carried out in the boundary layer on the plate with roughness element No. 3 were intended to study the deformation of the velocity diagram in the trailing-edge portion of the roughness element and at the flat surface of the plate, immediately behind the roughness element. The results of these measurements are shown in Fig. 2.

The measurements were carried out in all of the cases for identical free-stream velocities of W_∞ = 12.4 m/sec. In the section x = 254 mm, the velocity of the potential flow attains values close to the maximum. As we can see, the velocity diagram in this case corresponds to a turbulent flow regime. The section x = 261 mm is also found in the profile of the roughness element. The velocity diagram at this section is already somewhat different from the turbulent profile. Here the fact that the point of boundary-layer separation is near the section x = 261 mm makes itself felt. The velocity diagram at the section x = 266 mm, also located within the roughness element, indicates that the separation of the boundary layer has already taken place. In the following sections x = 271, 276, 281 and 289 mm we find that the velocity diagrams are deformed in the direction toward the turbulent profile; this leads to intensive mixing of the air within the separation zone (in analogy with the velocity diagram in the section beyond the rectangular roughness element [2]).

The figure shows that even at x = 284 mm, a significant velocity gradient appears at the wall, which indicates the origin of a new boundary layer after the separation of the old boundary layer from the element.

On the basis of the cited analysis of the results from the measurement of the velocities in the boundary layer, we can draw the conclusion that on a plate with a solitary roughness element the turbulent boundary layer retains its structure all the way to the point of separation. Beyond the point of separation a new turbulent boundary layer begins to form.

To verify the results of the analysis of the theoretical solution for the heat-transfer problem with respect to a plate with a single roughness element of arbitrary shape in the case of a constant heat flux, we carried out experiments to determine the transfer of heat from a plate with roughness element Nos. 1–3. The experimental data in this case are in good agreement with Eq. (12).

By measuring the force of the total aerodynamic resistance [drag] for a plate with a smooth surface, as well as for one with a roughness element, we were able to establish a quadratic relationship between the drag force and velocity.

Comparison of the results for plates with single roughness elements of wing profile and rectangular cross section [2] showed that for identical values of the drag force, the plate with the wing-profile roughness element exhibits the most intense heat transfer. In the latter case, the transfer of heat is intensified by the separation of the boundary layer, as well as by the increase in velocity, and perhaps also by the reduction in the thickness of the layer along the profile of the roughness element.

This investigation into the heat transfer of rough tubes with roughness elements in the form of diaphragms whose sections exhibit the shape of a wing profile has demonstrated the expediency of utilizing wing-profile roughness elements as heat-transfer intensifiers.

The periodically spaced roughness elements positioned along the length of the tube serve in this case to disrupt the boundary layer periodically, and to make the latter turbulent. We will assume that a new boundary layer of turbulent structure is formed behind each roughness element. Then, in analogy with a plate having a roughness element, we will find an elevated value for the heat-transfer coefficient behind each diaphragm, as well as at the initial segments.

Here it is easy to derive an expression for the calculation of the heat transfer of a rough tube in the

form

$$\frac{Nu_{av}}{Nu_{av\,s.t}} = \left(\frac{\frac{d}{t}}{\frac{d}{L}}\right)^{0.2} = n^{0.2}. \quad (13)$$

We can see from this expression that the heat-transfer law is identical for smooth and rough tubes. Thus

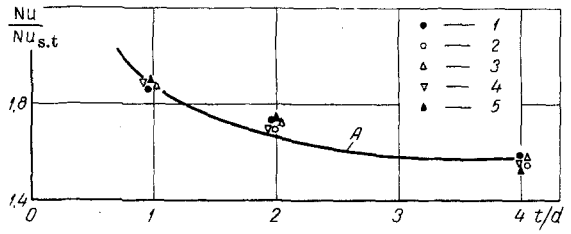

Fig. 3. Relationship $Nu/Nu_{s.t} = f(t/d)$ for rough tube with roughness element $z = z_{f_0} + 1.5\,z_{c_2}$, chord b = 12.5 mm: A) theoretical relation [7]; 1) Re_{av} = = 12 600; 2) 20 000; 3) 31 460; 4) 50 000; 5) 79 500.

for the turbulent flow region in the case of a rough tube we have $Nu_{av} \sim Re_{av}^{0.8}$, which is experimentally confirmed in [7], [8], et al.

Here we have also undertaken an experimental investigation into the heat transfer and resistance of rough tubes.

The test section was fabricated of copper tubing with an inside diameter of 25 mm and a length of 1000 mm. All of the tubes were first calibrated, and the roughness elements were then knurled on.

After all of the experiments were carried out, the test tubes were cut apart and the profiles produced by the knurling operation were measured.

To determine the effect of the shape, dimensions, and pitch of the knurled roughness elements on the heat transfer and aerodynamic resistance of the tubes, we investigated 1 smooth tube and 6 that had been roughened. The rough tubes exhibited the characteristics* shown in the table.

The processing of the experimental data gave us a criterial relationship to calculate the mean value of the Nusselt number and the average drag for rough tubes in the region in which the Reynolds number varied from $1.4 \cdot 10^4$ to $8 \cdot 10^4$.

For tube No. 1:

$$Nu_{av} = 0.0353\,Re_{av}^{0.8}, \quad \xi = \frac{1.43}{Re_{av}^{0.289}}. \quad (14)$$

For tube No. 2:

$$Nu_{av} = 0.0344\,Re_{av}^{0.8}, \quad \xi = \frac{7.5}{Re_{av}^{0.45}}. \quad (15)$$

For tube No. 3:

$$Nu_{av} = 0.0282\,Re_{av}^{0.8}, \quad \xi = \frac{11.35}{Re_{av}^{0.31}}. \quad (16)$$

*The notations for the profiles, as well as for their geometric dimensions, are based on the Simonov method of [4].

For tube No. 4:

$$Nu_{av} = 0.0875\,Re_{av}^{0.8}, \quad \xi = \frac{13.03}{Re_{av}^{0.5}}. \quad (17)$$

For tube No. 5:

$$Nu_{av} = 0.155\,Re_{av}^{0.655}, \quad \xi = \frac{6.92}{Re_{av}^{0.425}}. \quad (18)$$

For tube No. 6:

$$Nu_{av} = 0.0251\,Re_{av}^{0.8}, \quad \xi = \frac{0.136}{Re_{av}^{0.0968}}. \quad (19)$$

In these formulas the mean logarithmic temperature difference is calculated from the formula

$$\Delta t_l = \frac{t_{out} - t_{in}}{\ln \frac{t_w - t_{in}}{t_w - t_{out}}},$$

while the equivalent diameter

$$d_{equiv} = \sqrt{\frac{4V}{\pi L}}.$$

As we can see, in the formula for Nu_{av} for tubes Nos. 1–3 and 6 the average Nusselt number is 0.8 of the Reynolds number, i.e., we find the same quantitative relationship as for smooth tubes in the turbulent region. With regard to the exponent in formulas (11) and (12) for Nu_{av}, here we can say that we see the influence of the stagnant zone behind the element with a reduced value for the heat-transfer coefficient in conjunction with the short segment between elements separated through a distance of 50 mm. An analogous phenomenon was found on the plate behind a rectangular roughness element more than 2 mm in height. The greatest height of the roughness element in knurled tubes Nos. 4 and 5 is 2.4 mm (measured after the tubes were cut apart).

We see from formulas (14)–(19) for the drag coefficient that the law governing the change in resistance for all of the investigated tubes is different; this serves to confirm the Shevelev [6] conclusion that the resistance curves

$$\xi = f(Re_{av})$$

may differ in shape, depending on the roughness characteristics. The quadratic resistance of the tubes, derived in the Nikuradse experiments, is only a special case among the various relationships. The law governing the resistance of a rough tube in final analysis is defined by the relationship between the resistance of the roughness-element shape and the frictional drag which, in turn, is made up of the frictional drag exhibited by the smooth segments and by the roughness element.

Figure 3 shows the comparison of the approximate theoretical evaluation of rough-tube heat transfer with the result of an experimental determination of heat transfer from a tube with roughness elements exhibiting a profile $z = z_{f_0} + 1.5\,z_{c_2}$ for various values of the pitch t/d.

The resulting experimental points in the interval of pitch variation and of a Reynolds-number range of

$12.9 \cdot 10^3 \leq Re \leq 71.3 \cdot 10^3$ are in satisfactory agreement with relationship (13). It should be borne in mind that formula (13) does not take into consideration the heat-transfer coefficient at the actual roughness element.

The experimental data derived by Nunner [8] are also satisfactorily described by Eq. (13). Thus, for a tube with half-cylinder profile rings 2 mm in height, the quantity $Nu_{av}/Nu_{av\ s.t}$, calculated according to formula (13), amounts to:

$$\text{for } z = 6 \text{ rings, } \frac{Nu_{av}}{Nu_{av\ s.t}} = 1.48;$$

$$\text{for } z = 24 \text{ rings, } \frac{Nu_{av}}{Nu_{av\ s.t}} = 1.91.$$

According to the Nunner experimental data for $Re_{av} = 3 \cdot 10^4$, the quantity $Nu_{av}/N_{uav\ s.t}$ is equal to 1.43 and 2, respectively.

Finally, we evaluate the effectiveness of the investigated rough tubes. The results from the calculation of the effectiveness of a smooth tube and of the roughened tubes are shown in Fig. 4. The comparative evaluation is carried out on the basis of the energy factor introduced by Kirpichev. In the work of Antuf'ev [5], the following expressions are used for the determination of the energy factor E:

$$E = \frac{\alpha_{av}}{N_0}, \tag{20}$$

$$N_0 = h_{loss} W_{av} \frac{f}{F}. \tag{21}$$

It follows from Fig. 2 that the highest effectiveness from among the various tubes studied is exhibited by tubes Nos. 2 and 4. Moreover, the tube with a roughness element whose chord is b = 16.6 mm (No. 4) is more effective than the tube with a roughness element of identical profile, but with a smaller chord, i.e., b = 12.5 mm (No. 2).

The heat-transfer coefficient for the roughened tube No. 4 under conditions of identical expenditures of energy for the propulsion of the air (N_0) is greater by a factor of 1.42 than for a smooth tube. It is evident that the area of the heat-transfer surface of a rough tube, all other conditions being equal, will be smaller by 42% than the surface area of a smooth tube.

NOTATION

$\theta = \Delta t = t_w - t_0$ is the variable temperature head; t_w is the wall temperature; t_0 is the flow temperature; W is the specified longitudinal velocity at the outer boundary of the layer; q_w is the heat flux; δ_t is the thickness of the thermal boundary layer $\delta_t^{**} = \int_0^{\delta_t} \frac{W_x}{W}\left(1 - \frac{t_w - t}{t_w - t_0}\right) dy$; t is the temperature in the thermal boundary layer; W_x is the velocity in the hydrodynamic boundary layer; $Re_t^{**} = W\delta_t^{**}/\nu$; $Nu_x = \alpha x/\lambda$; $\alpha = q_w/\theta$ is the heat-transfer coefficient; $Re_x = W_\infty x/\nu$; $Pr = \gamma c_p \nu/\lambda$; γ is the specific weight; ν is the kinematic viscosity coefficient; λ is the thermal conductivity; c_p is the specific heat capacity; W_∞ is the velocity of incoming flow; Nu_{av} is the mean Nusselt number for rough tubes; $Nu_{av\ s.t}$ is the mean Nusselt number for

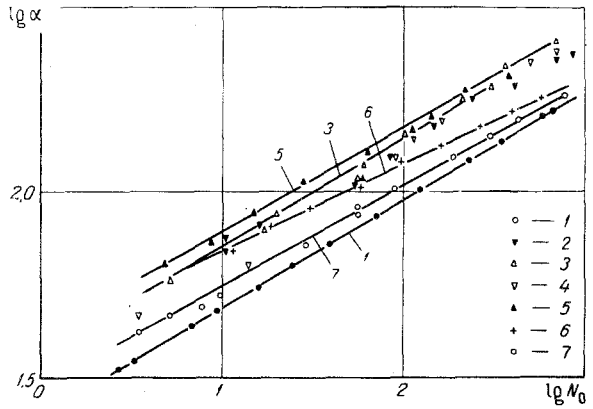

Fig. 4. Comparison of efficiency in smooth and rough tubes with various properties of roughness element: 1) smooth tube; 2) No. 1; 3) No. 2; 4) No. 3; 5) No. 4; 6) No. 5; 7) No. 6.

smooth tubes; d is the tube diameter; t is the pitch of the roughness elements; L is the tube length; α_{av} is the mean heat transfer coefficient; Re_{av} is the mean Reynolds number; W_{av} is the average of the air-flow rate in the tube; d_{equiv} is the equivalent diameter; ξ is the mean resistance coefficient; Δt_l is the mean-logarithmic temperature head; t_{in} is the inlet temperature; t_{out} is the outlet temperature; V is the volume of the knurled tube portion; E is the energy factor; N_0 is the energy spent on resistance per unit time per unit heat-transfer surface; h_{loss} is the head loss; f is the tube section; F is the heat-transfer surface; b is the profile chord.

REFERENCES

1. G. S. Ambrok, ZhTF, vol. XXVII, no. 9, 1957.

2. V. M. Buznik, V. N. Bandura, and G. A. Artemov, collection: Shipbuilding and Marine Construction [in Russian], no. 4, 3, 1966.

3. V. M. Buznik, G. A. Artemov, V. N. Bandura, and A. M. Fedorovskii, IFZh [Journal of Engineering Physics], vol. XI, no. 1, 1966.

4. L. A. Simonov, Prikladnaya matematika i mekhanika, vol. XI, no. 1, 1947.

5. V. M. Antuf'ev, Energomashinostroenie, no. 5, 1964.

6. F. A. Shevelev, An Investigation into the Fundamental Hydraulic Quantitative Relationships of Turbulent Motion in Tubes [in Russian], Gosizdat po stroitel'stvu i arkhitekture, 1953.

7. R. Koch, VDI—Forschung, no. 469, Düsseldorf, 1958.

8. W. Nunner, VDI—Forschung, no. 455, 1956.

3 July 1967

Makarov Shipbuilding Institute, Nikolaev